



**Enhancing the optical properties of semiconductor nanostructures with
metal films and surface plasmons**

Prof. Dan Rich

Department of Physics

Ben-Gurion University of the Negev, Beer-Sheva, Israel

Collaborators:

Yevgeni Estrin (Ph.D. student, BGU)

Samples were provided by:

Dr. Andrey V. Kretinin (Weizmann Institute of Science, Israel)

Dr. Hadas Shtrikman (Weizmann Institute of Science, Israel)

Dr. Stacia Keller (Univ. California, Santa Barbara, USA)

Prof. Steve DenBaars (Univ. California, Santa Barbara, USA)

Prof. Amir Sa'ar (Hebrew University, Israel)

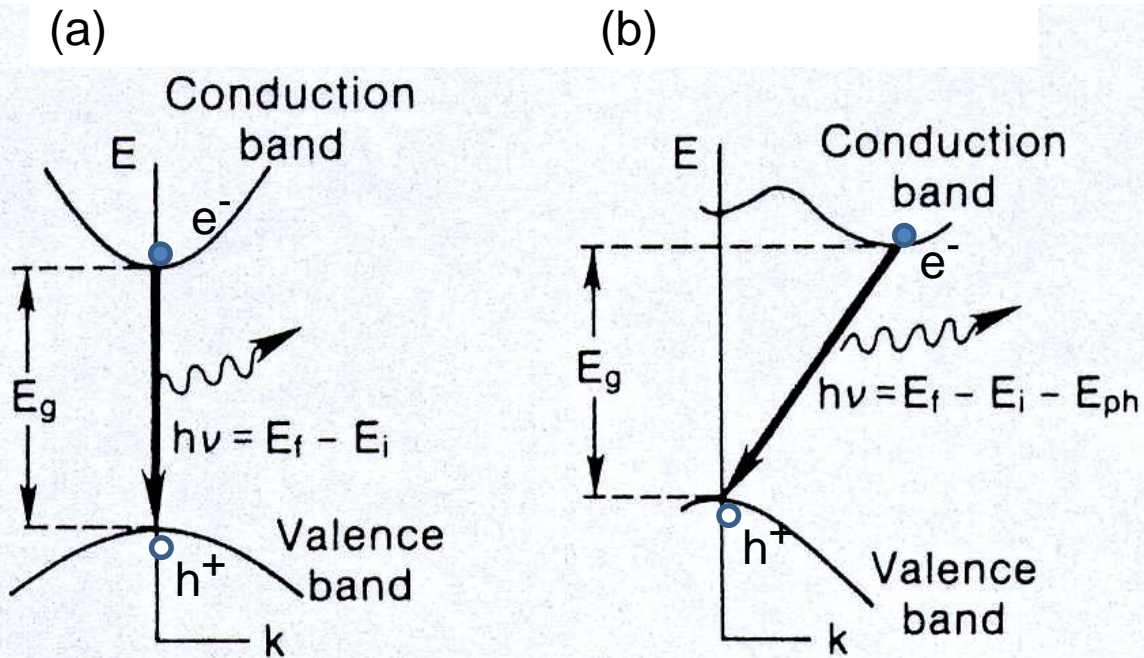


An important focus in nanostructures is the design of plasmonic metal/semiconductor composite structures to obtain novel optical device properties for applications in biological labeling/sensing, light-emitting diodes, lasers, and solar cells.

Outline of Talk

1. Growth of **GaAs/AlAs/GaAs core-shell nanowires (NWs)**, **InGaN/GaN QWs**, and **Si nano-crystals (SiNCs)** (i.e., quantum dots (QDs))
2. Deposition of thin metal films: Gold, Silver and Aluminum films on the three material systems with dimensionalities of (i) QWs, (ii) NWs, and (iii) QDs
3. Spatially, Spectrally, and temporally-resolved cathodoluminescence (CL): *e*-beam probe and easy penetration of thin metal films
4. Assess coupling of **excitons** (*e-h* pairs) to **surface plasmon polaritons (SPPs)**
5. Measure changes in the spontaneous emission rate (**SER**) of excitons in the nanowires and quantify the Purcell Enhancement Factor (F_p)

Semiconductor Physics



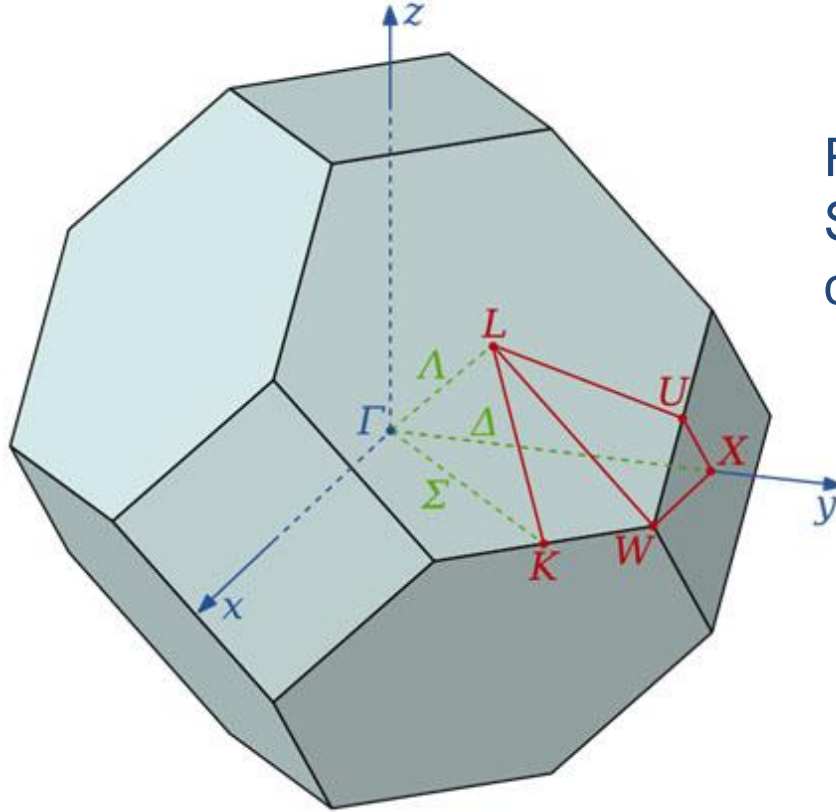
Exciton (e-h pair)

GaAs, GaN, InGaN

Silicon, Germanium

FIG. 1. Energy transitions in (a) direct and (b) indirect gap semiconductors between initial states E_i and final states E_f . For indirect transitions (b) the participation of a phonon (E_{ph}) is required.

The face centered cubic (fcc) Brillouin Zone

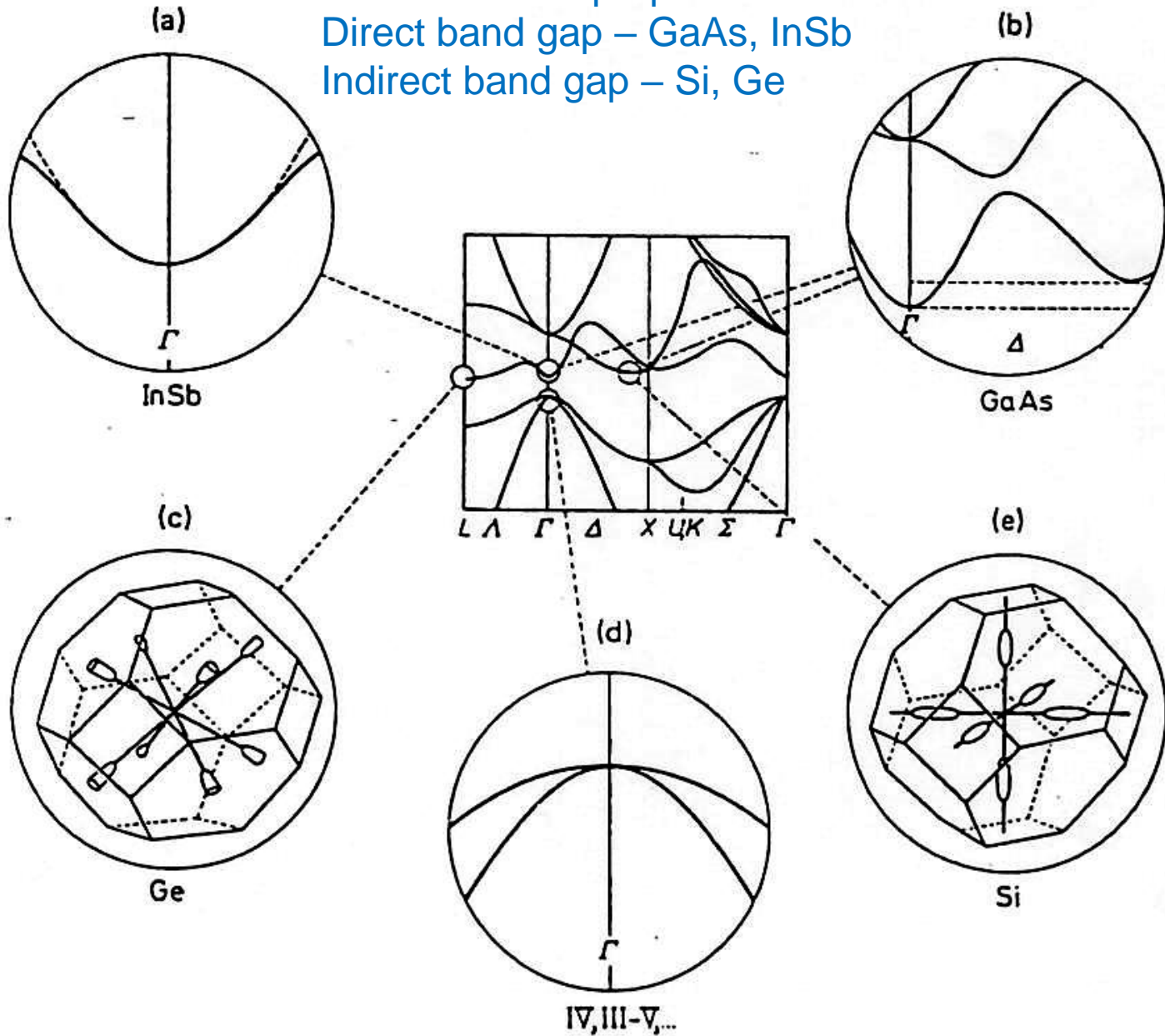


Relevant Semiconductors:
Si, Ge, GaAs and many III-V
compounds

Special symmetry points:

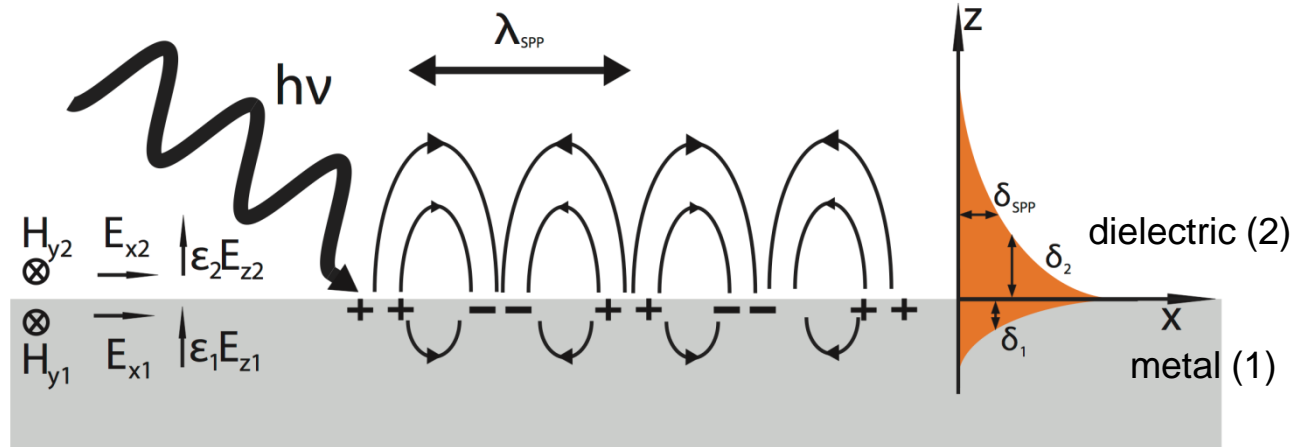
$$\begin{aligned} X &= (0, 1, 0) 2\pi/a, & L &= (1/2, 1/2, 1/2) 2\pi/a, \\ K &= (3/4, 3/4, 0) 2\pi/a, & W &= (1/2, 1, 0) 2\pi/a, \\ U &= (1/4, 1, 1/4) 2\pi/a \end{aligned}$$

Band structure properties
Direct band gap – GaAs, InSb
Indirect band gap – Si, Ge





Basics of Surface Plasmon Polaritons (SPPs)

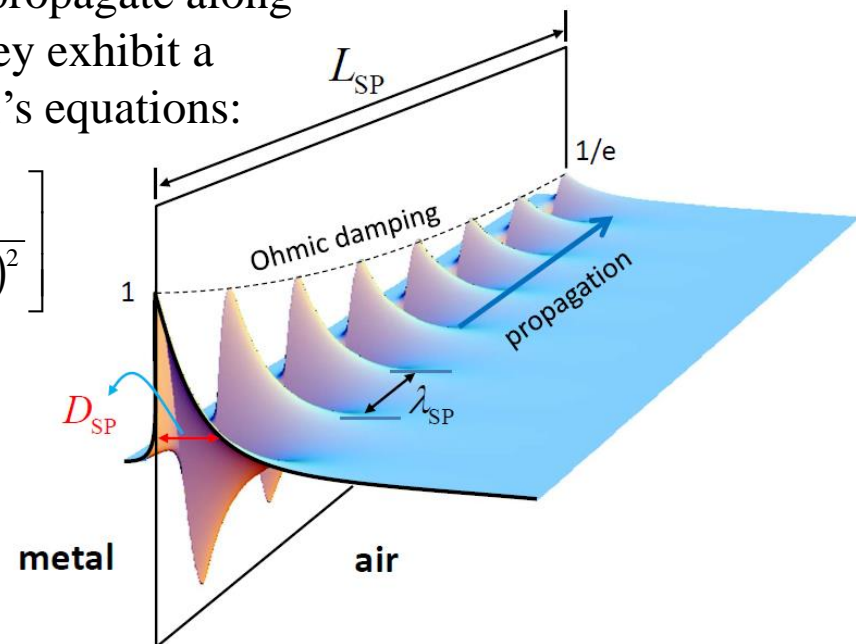


SPPs are oscillations in the charge density that propagate along the interface between a metal and dielectric. They exhibit a complex wavevector from solutions to Maxwell's equations:

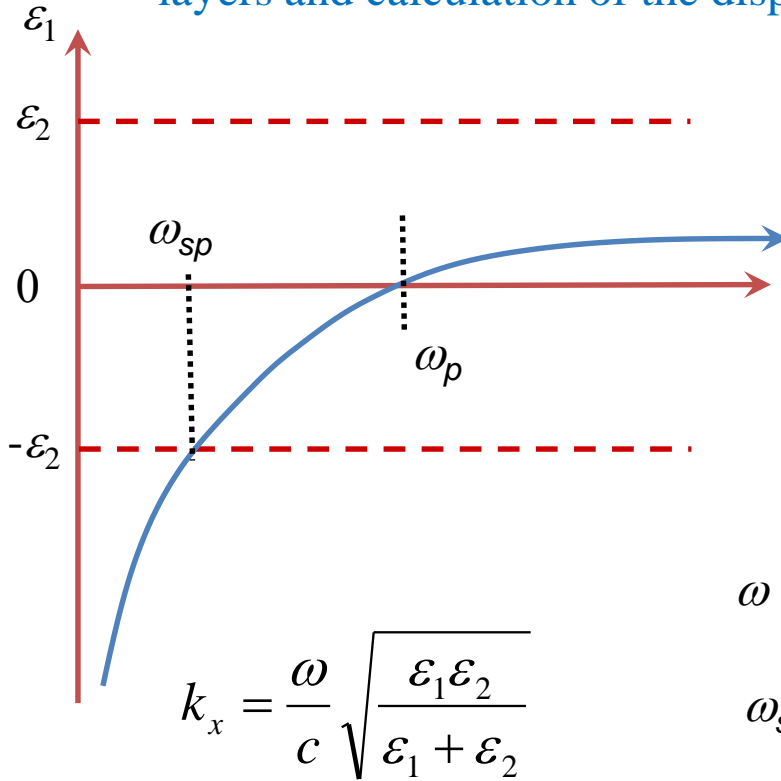
$$k_x = k'_x + ik''_x = \left[\frac{\omega}{c} \left(\frac{\epsilon'_1 \epsilon_2}{\epsilon'_1 + \epsilon_2} \right)^{1/2} \right] + i \left[\frac{\omega}{c} \left(\frac{\epsilon'_1 \epsilon_2}{\epsilon'_1 + \epsilon_2} \right)^{3/2} \frac{\epsilon''_1}{2(\epsilon'_1)^2} \right]$$

$$L_{SP} = \frac{1}{2k''_x} \quad (\text{Propagation length})$$

$$z_i = \frac{\lambda}{2\pi} \left(\frac{|\epsilon'_1| + \epsilon_2}{\epsilon_i^2} \right)^{1/2} \quad (\text{E-field decay length})$$



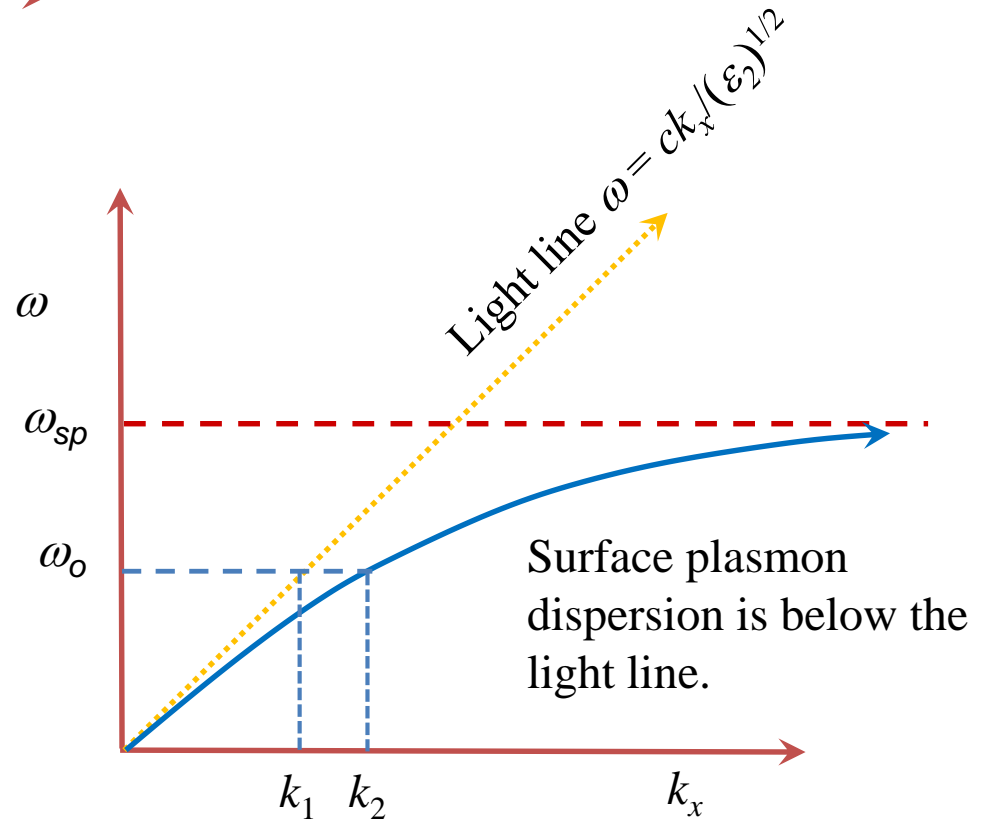
Examination of the dielectric constants for both the metal (ϵ_1) and dielectric (ϵ_2) layers and calculation of the dispersion relation $\omega(k_x)$ for surface plasmons.



1) For small ω , $\epsilon_1 \rightarrow -\infty$ and $k_x \approx (\omega/c)(\epsilon_2)^{1/2} = \omega/v_d$

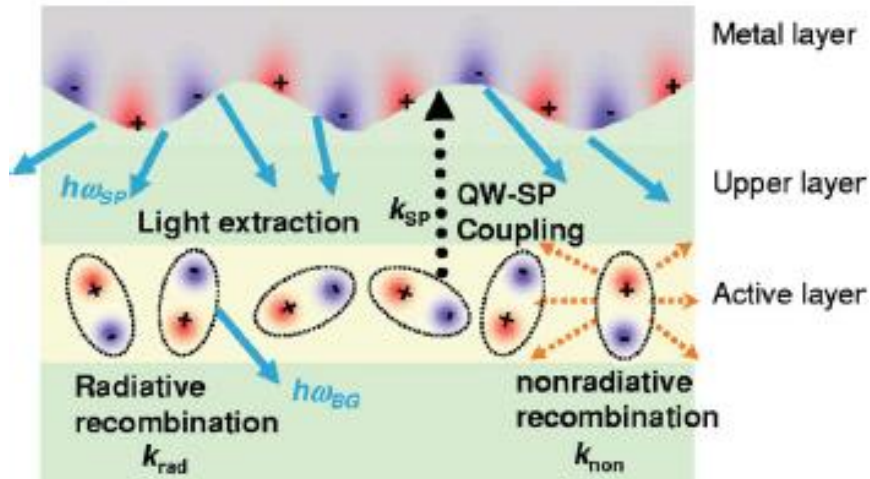
2) At $\omega = \omega_{sp}$, $\epsilon_1 \rightarrow -\epsilon_2$ (from below) and $k_x \rightarrow +\infty$

$$n^2 = \epsilon_1(\omega) = 1 - \frac{\omega_p^2}{\omega^2}$$

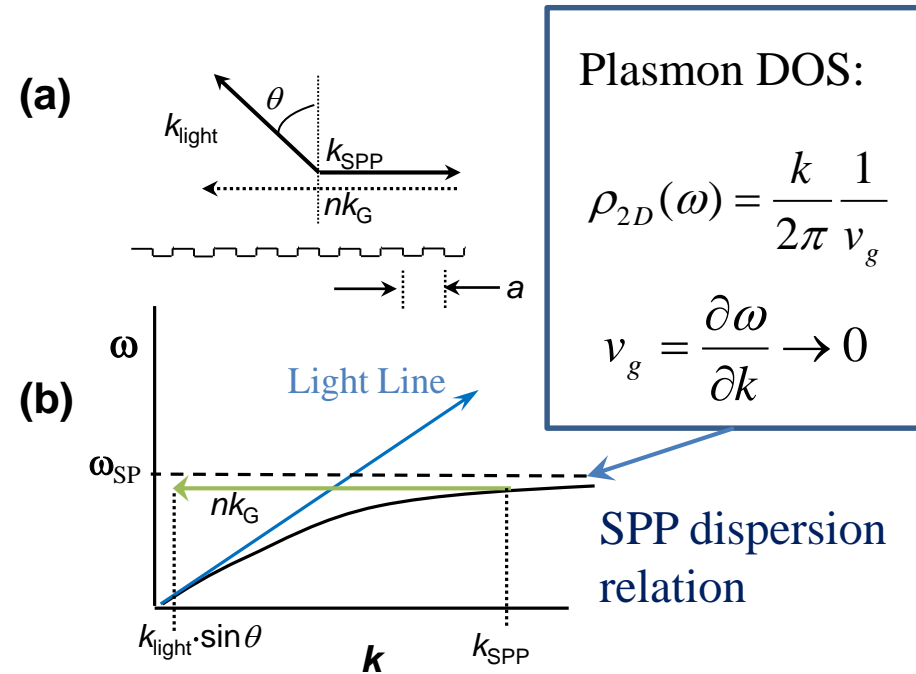


In general, the phase velocity of SPPs ($v_{ph} = \omega/k$) is less than that of light in the dielectric adjacent to a metal film.

- 1) Exciton ($e-h$ pair) to SPP coupling (quantum well, wire or dot)
- 2) SPP conversion to a photon



Model of the exciton-SPP coupling mechanism. (K. Okamoto et al. APL **87**, 071102 (2005))



The decoupling of SPPs into light is described by the kinematic equation: $\text{Re}[k_{\text{SPP}}(\omega)] - nk_G = (\omega/c)\sin(\theta)$.

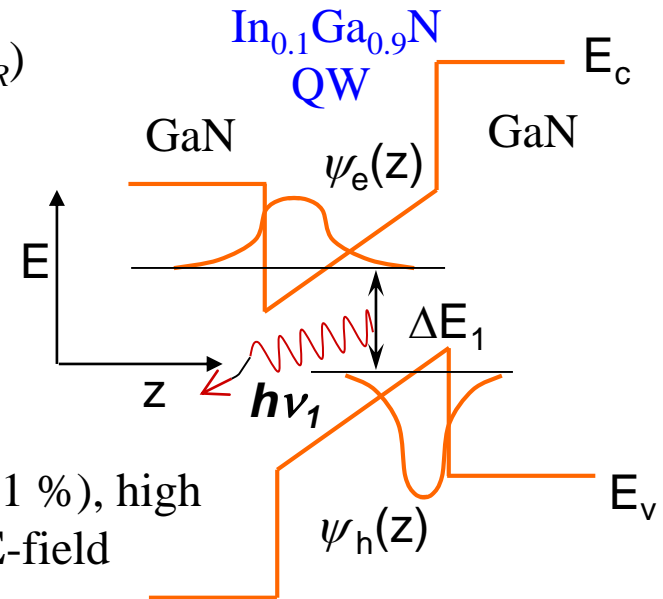
- Scattering occurs by the surface/interface roughness or grain boundaries of the polycrystalline metal film.
- Momentum change associated with the scattering enables a matching with the ω vs k light dispersion relation.
- Roughness is a superposition of many gratings with different k_G .



Challenges and Motivation for increasing the SER in quantum heterostructures / nanostructures

1. $\text{In}_x\text{Ga}_{1-x}\text{N}/\text{GaN}$ QWs used for LEDs / Lasers

- Growth on *c*-plane (0001) Sapphire : Conventional MOCVD techniques lead to a high threading dislocation density ($\sim 10^8 - 10^9 \text{ cm}^{-2}$) and V-pit defects, owing to the large lattice mismatch between wurtzite (hexagonal) GaN and Sapphire.
- Large piezo-electric fields ($\sim 10^6 \text{ V/cm}$) lead to a reduced oscillator strength.
- Thus, the non-radiative recombination rate ($R_{NR} = 1/\tau_{NR}$) will compete with the radiative rate ($R_R = 1/\tau_R$).
- For metal-coated QWs, coupling between excitons and SPPs may lead to a larger R_R for improved IQE for opto-electronics and overcoming “green gap” in LED performance.



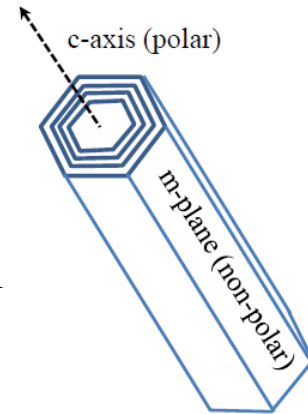
Large strain ($\sim 1\%$), high piezoelectric \mathbf{E} -field



Challenges and Motivation for increasing the SER in quantum heterostructures / nanostructures

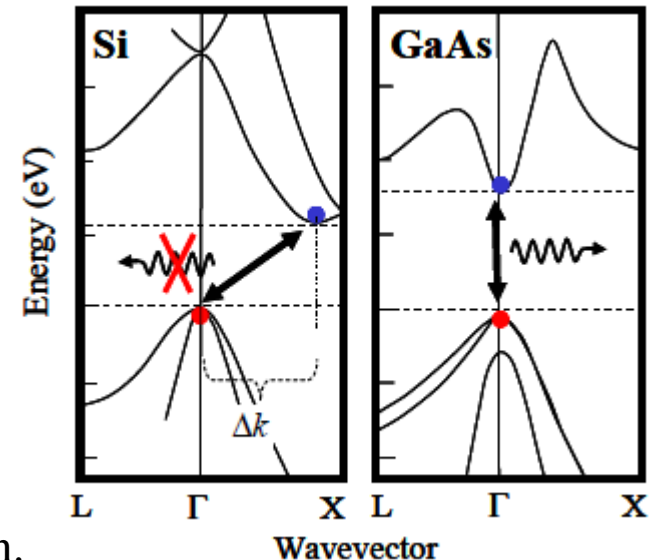
2. III-V core-shell nanowires possess a large surface recombination velocity (S).

- For bare GaAs wires, $\tau_{NR} = d/2S \approx 10^{-12}$ s for a NW diameter (d) of 30 nm and $S = 10^6$ cm/s.
- For GaN wires, $S \sim 10^4$ cm/s, but the piezoelectric fields can limit the IQE, as seen for the QWs.



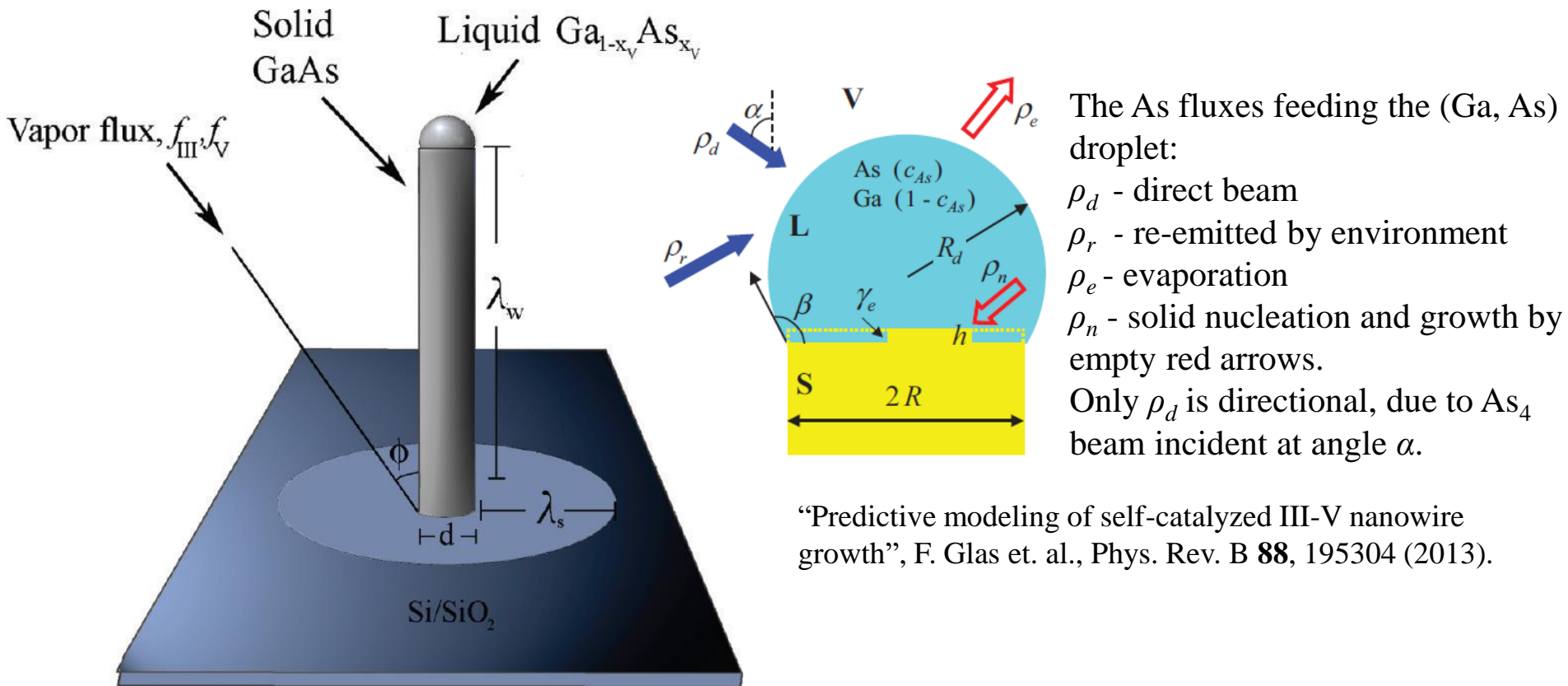
3. Si Nanocrystals (SiNCs)

- Bulk Si is an indirect bandgap material which leads to long $e-h$ lifetimes (\sim ms) due to the need for momentum conservation (phonons); limits usefulness in light emitters.
- However, for small SiNCs ($D \sim 3$ nm), Momentum conservation is partially relaxed due to Heisenberg uncertainty principle: $\Delta k \sim 1/D$.
- Quantum confinement leads to *quasi-direct* transition.
- Coupling of excitons to SPPs for metal-coated nanostructures for larger QE.



MBE Growth of GaAs nanowires: Vapor-Liquid-Solid (VLS) self-assisted catalyst-free growth

Gallium droplets are formed on the surface of the wafer which, on reaching a critical size, become supersaturated and begin nanowire growth.



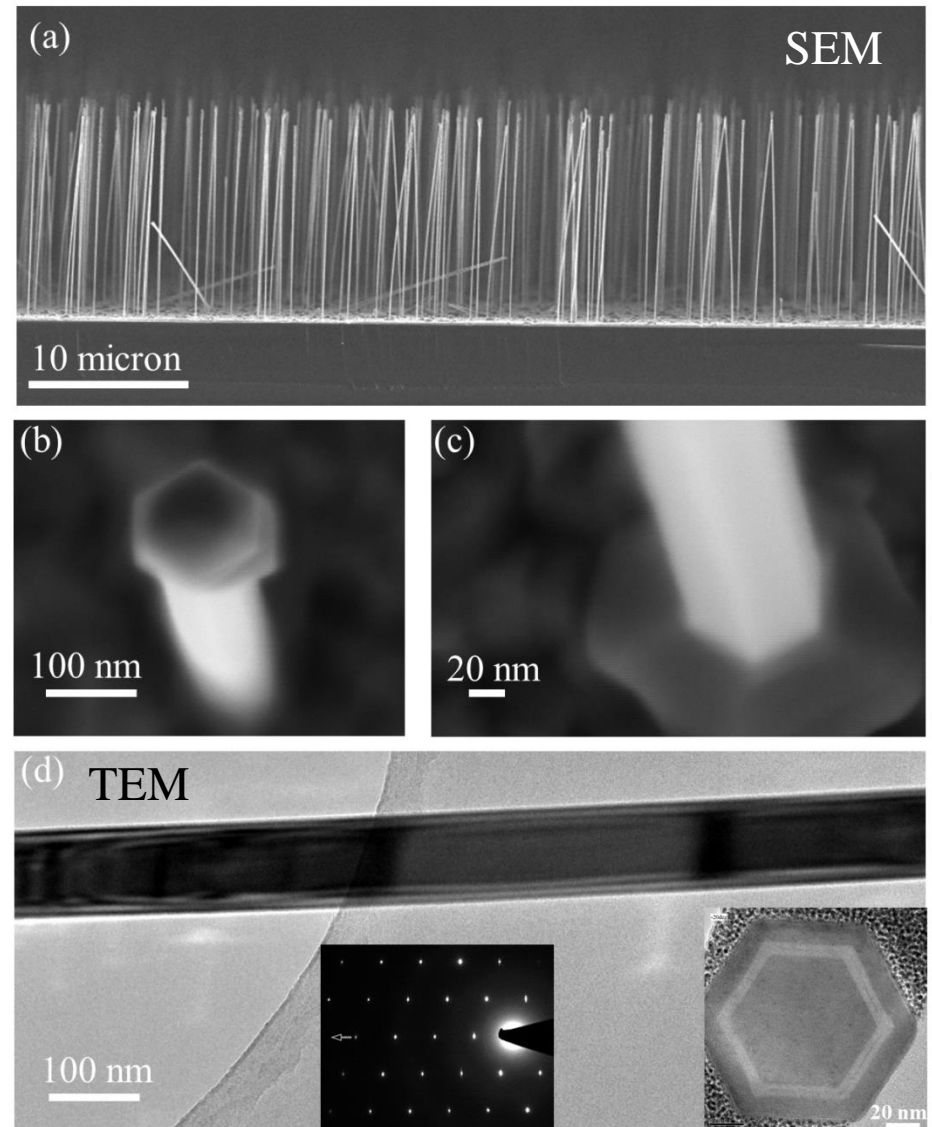
“Predictive modeling of self-catalyzed III-V nanowire growth”, F. Glas et. al., Phys. Rev. B **88**, 195304 (2013).

“Structural Phase Control in Self-Catalyzed Growth of GaAs Nanowires on Si(111)”, P. Krogstrup, R. Popovitz-Biro, E. Johnson, M. Hannibal Madsen, J. Nygård and H. Shtrikman. Nano Letters **10**, 4475 (2010).



Nanowire growth:

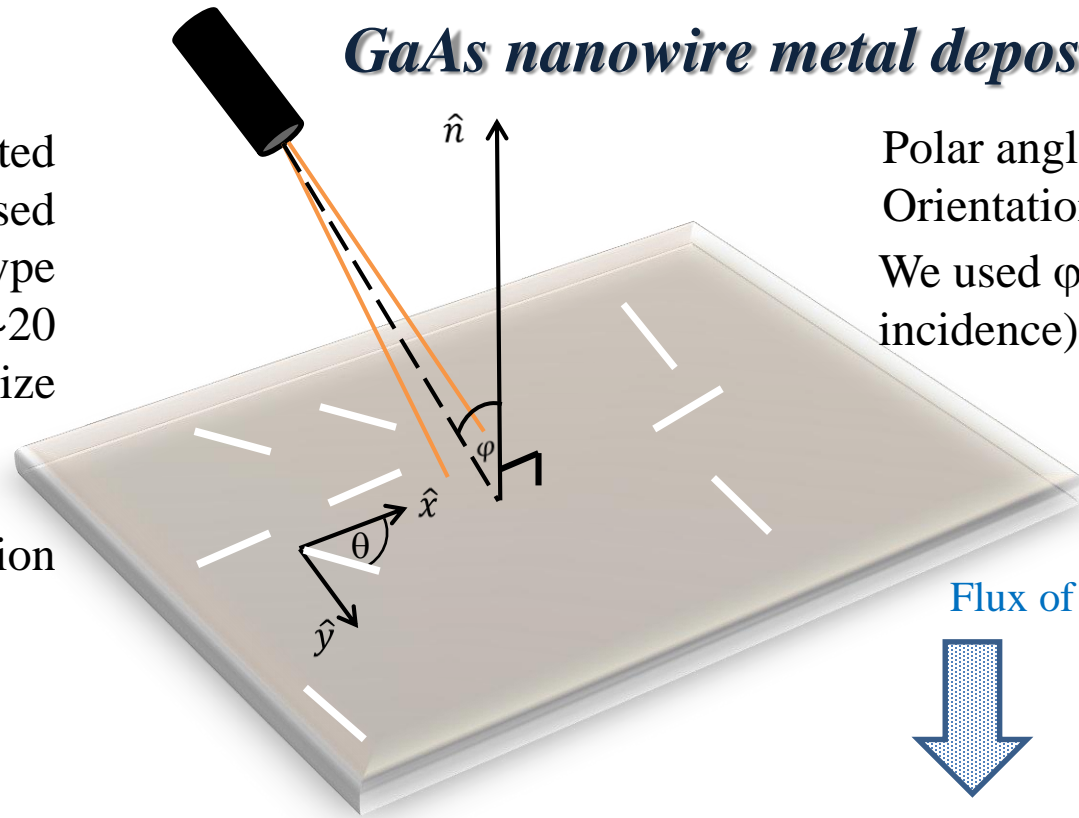
- MBE growth of GaAs/AlAs/GaAs core-shell nanowires using the self-assisted VLS method
- Substrate: Si(111) with native oxide layer
- Water removal at ~ 200 °C, outgassing at ~ 600 °C
- Growth: initiated by condensation of Ga, $T_G \approx 640$ °C, and a V/III (As_4/Ga) ratio of ~ 100
- Uniform ~ 6 nm AlAs shell and ~ 12 nm GaAs capping layer, $T_G \approx 520$ °C
- Wire growth direction: $\langle 111 \rangle$, hexagonal shape with $\{011\}$ facets
- Uniform diameter of ~ 100 nm, ~ 12 μm length, aspect ratio ~ 100 , without tapering, and a pure zinc-blende structure (TEM).





GaAs nanowire metal deposition

- Nanowires were harvested and randomly dispersed onto heavily doped p -type Si wafers coated with ~ 20 nm-thick Al (to minimize charging in CL).
- Au and Al evaporation thickness (t_0) ~ 20 nm



Polar angle (φ)
Orientation angle (θ)
We used $\varphi = 0^\circ$ (normal incidence).

1. Nanowire $\varphi = 0$, any θ .

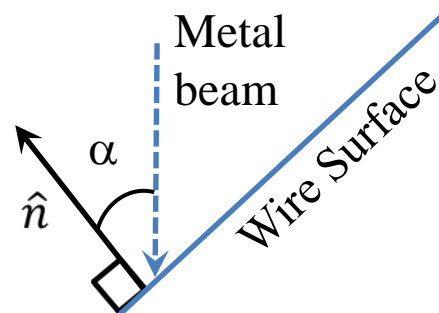


2. Nanowire $\varphi > 0$, $\theta = 0$.

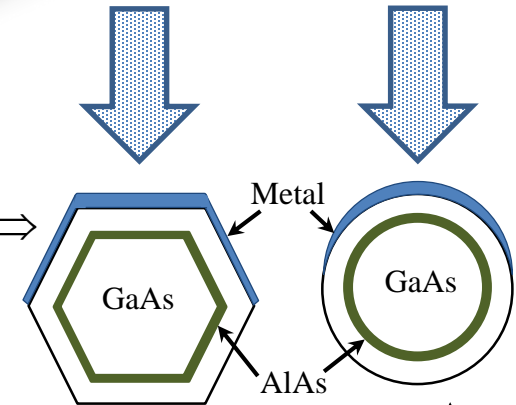


Si(111) p^+ -doped

$$t = t_0 \cos \alpha \Rightarrow$$



Flux of metal atoms

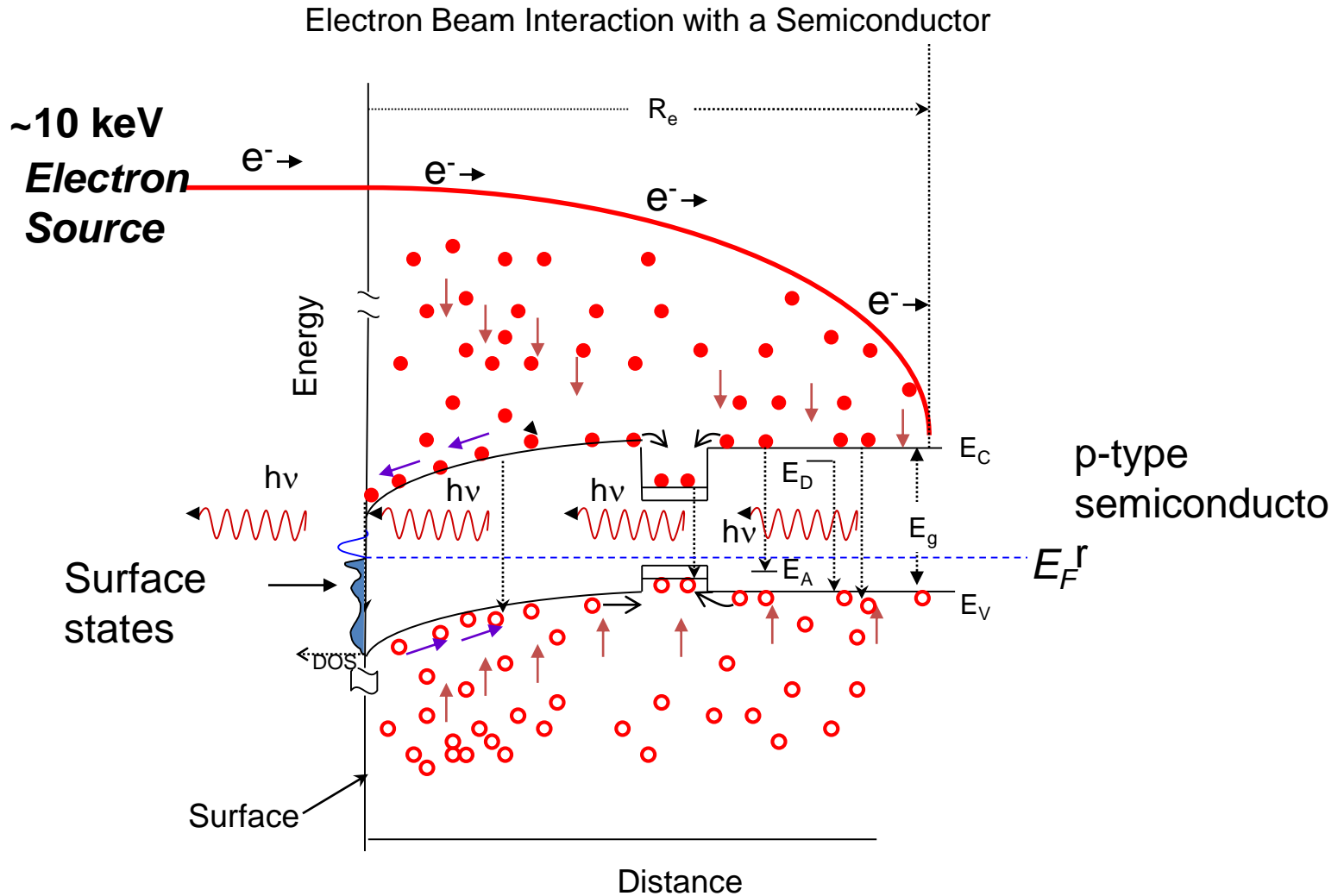


(Side view)

Tapered thickness
or crescent shape
in cross-section



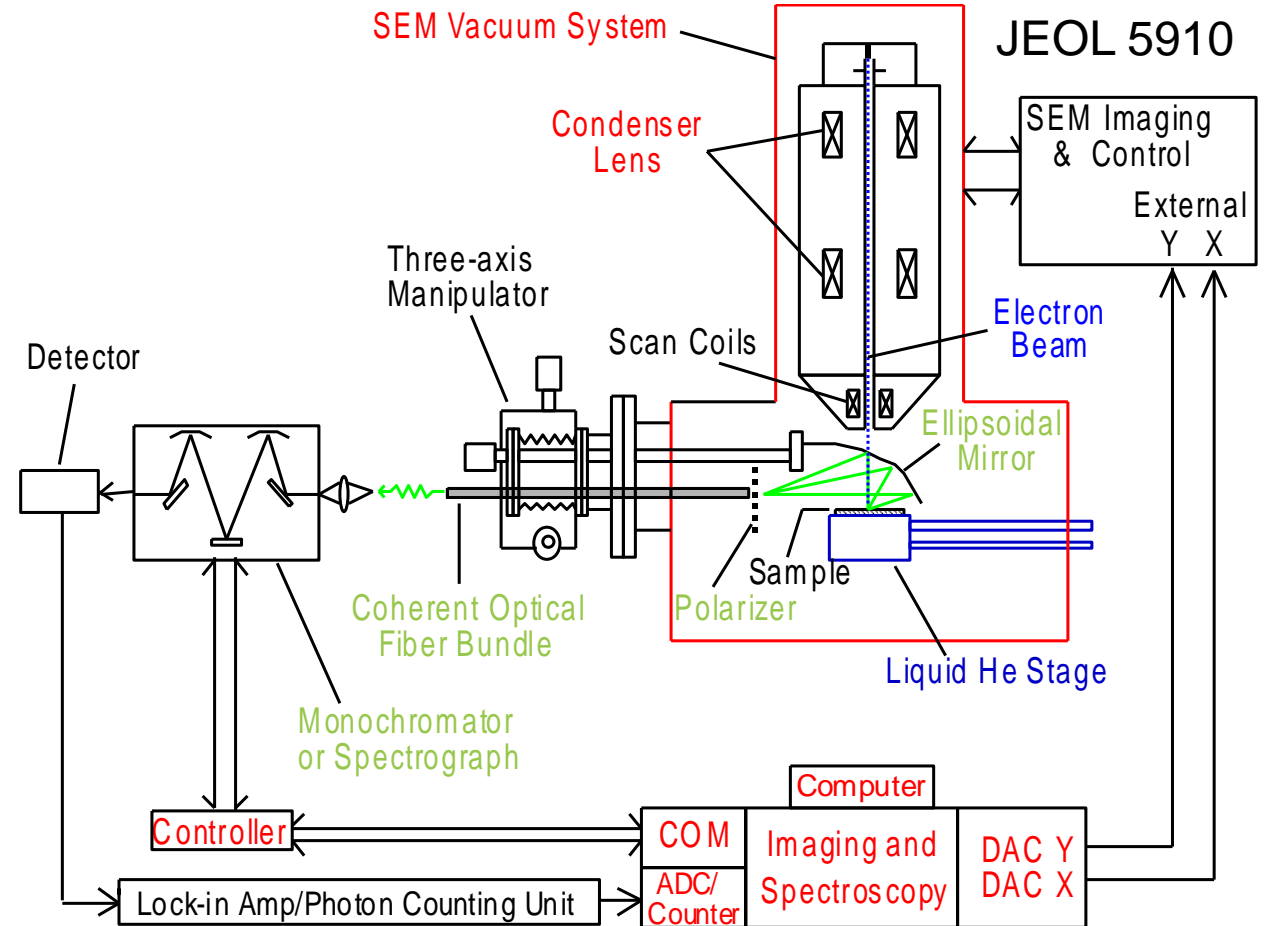
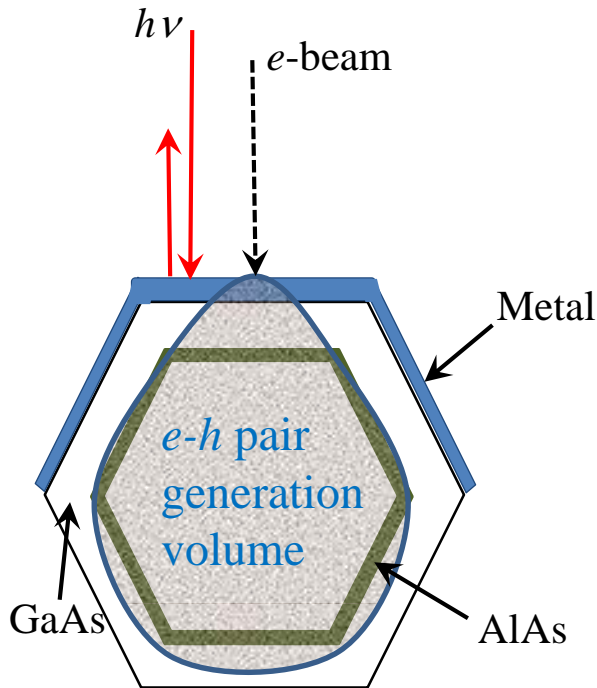
What is Cathodoluminescence (CL)?





Cathodoluminescence (CL) system

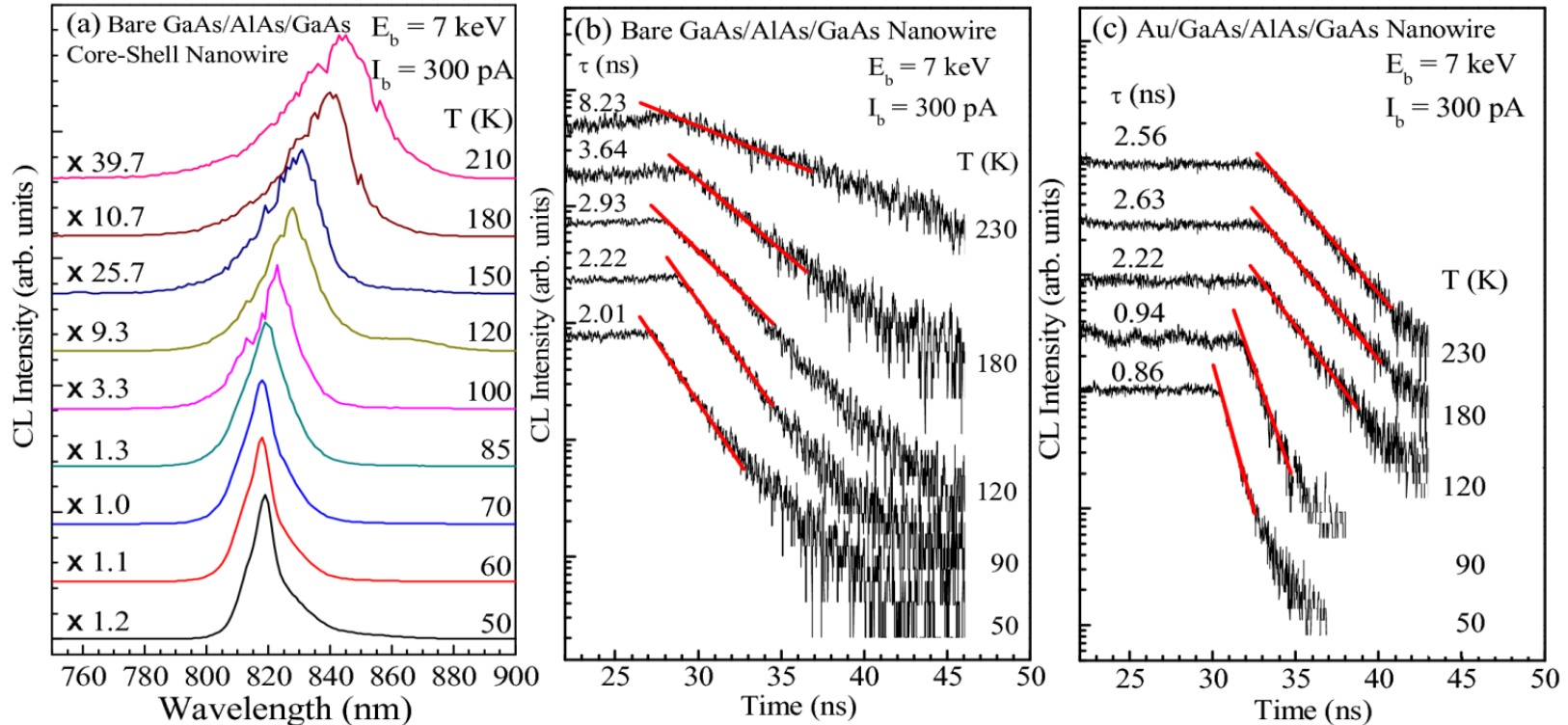
Advantage of e -beam over laser excitation for metal covered nanostructures:



Schematic diagram of optical collection system and data acquisition setup in our CL system.



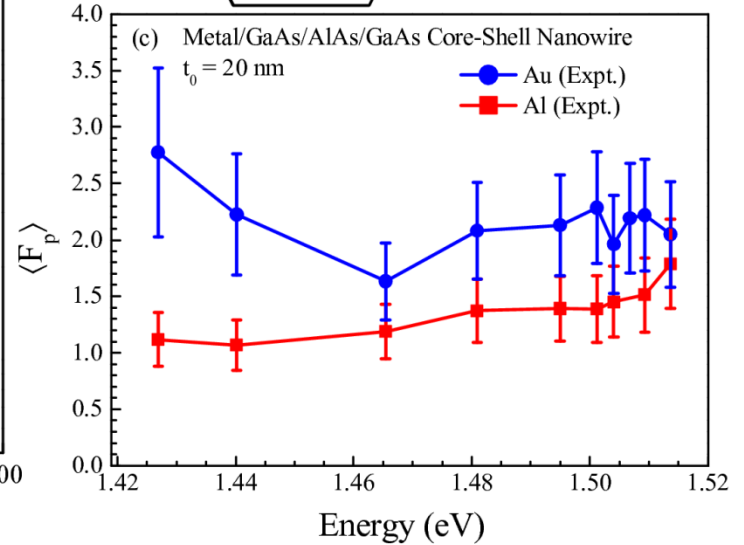
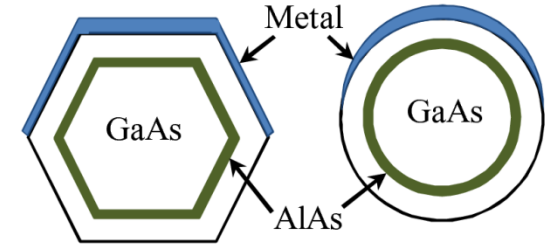
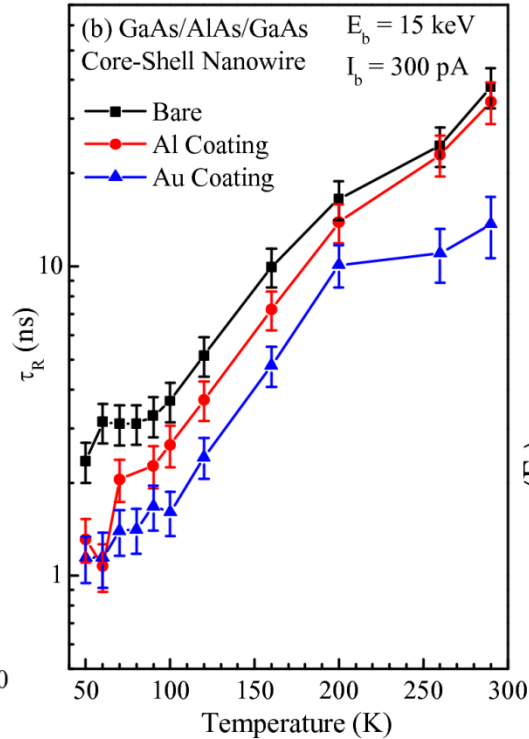
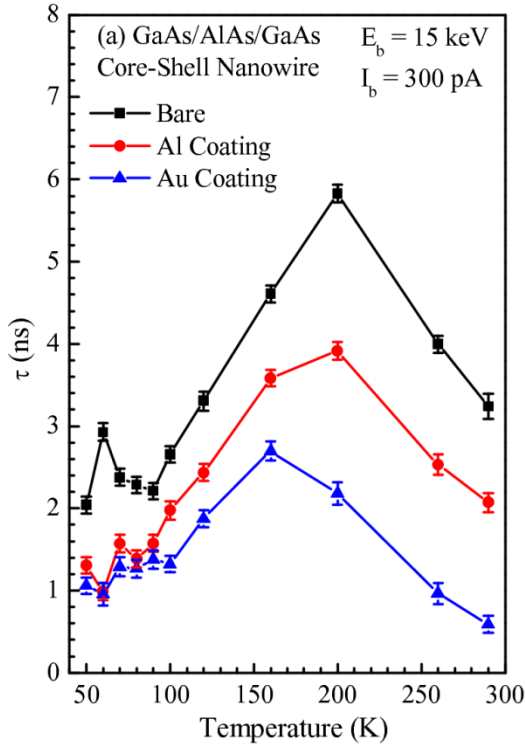
Temperature-dependent CL spectroscopy and time-resolved CL



- GaAs NBE emission for e -beam excitation of a single nanowire (broadening, red-shift, and reduced intensity as T increases).
- Carrier lifetimes (τ) from slope of CL transients (single exponential fits).
- Deposition of Gold reduces τ at all temperatures relative to bare and Aluminum films.



Temperature dependence of $\tau_R(T)$ from $\tau(T)$ and the Purcell Factor (F_p)



We have extracted $\tau_R(T)$ from $\tau(T)$ and $I(T)$.

Radiative efficiency:
$$\eta(T) = \frac{\tau(T)}{\tau_R(T)} = \frac{I(T)}{I_0}$$

I_0 is the saturation CL intensity at low temp.

$$\langle F_p(\omega) \rangle = \tau_{R(bare)} / \tau_{R(metal)}$$

$\hbar\omega_{\text{GaAs}} \approx 1.510 \text{ eV}$ at $T = 50 \text{ K}$

Au/GaAs: $\hbar\omega_{SP} \approx 1.804 \text{ eV}$

Al/GaAs: $\hbar\omega_{SP} \approx 2.700 \text{ eV}$

(From ω vs k dispersion calculation)

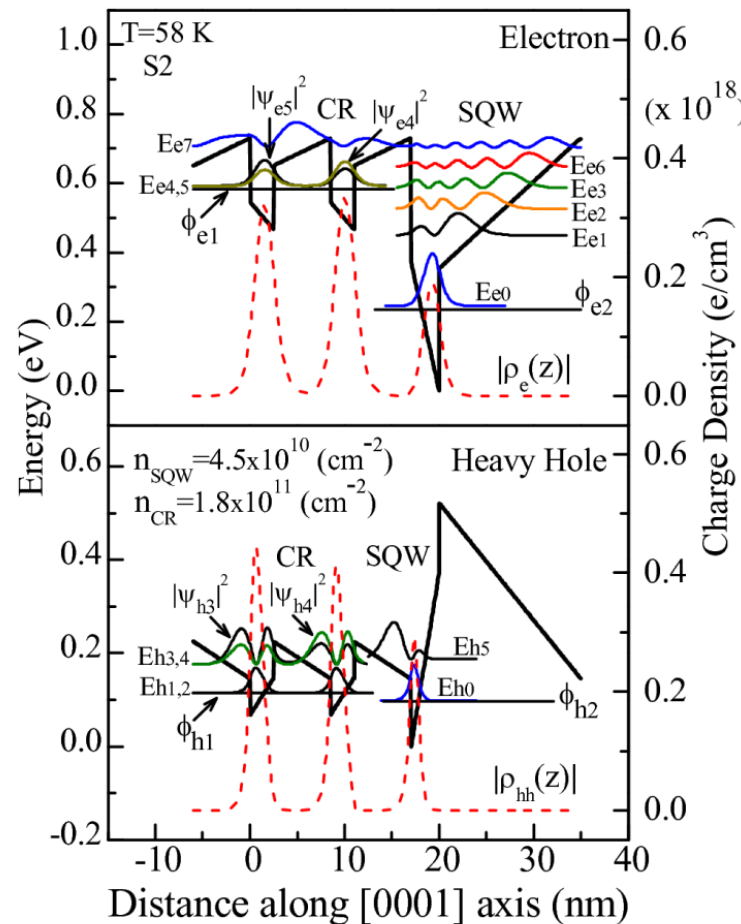
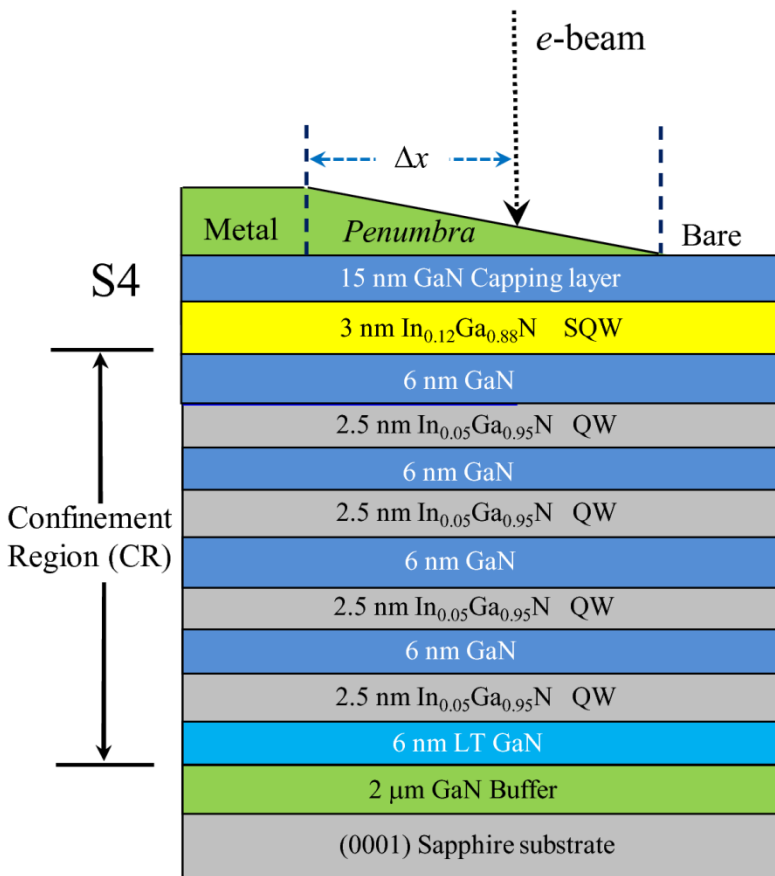
Therefore, we expect $F_p(\text{Au}) > F_p(\text{Al})$



Time-resolved CL and CL imaging of InGaN/GaN QWs with metal films for exciton-to-SPP coupling

MOCVD-grown $\text{In}_x\text{Ga}_{1-x}/\text{GaN}$ MQW Samples

Metal films: Ag, Au, and Al, thickness of 20 nm



Calculation of Energy states and wavefunctions for confined electrons and holes:

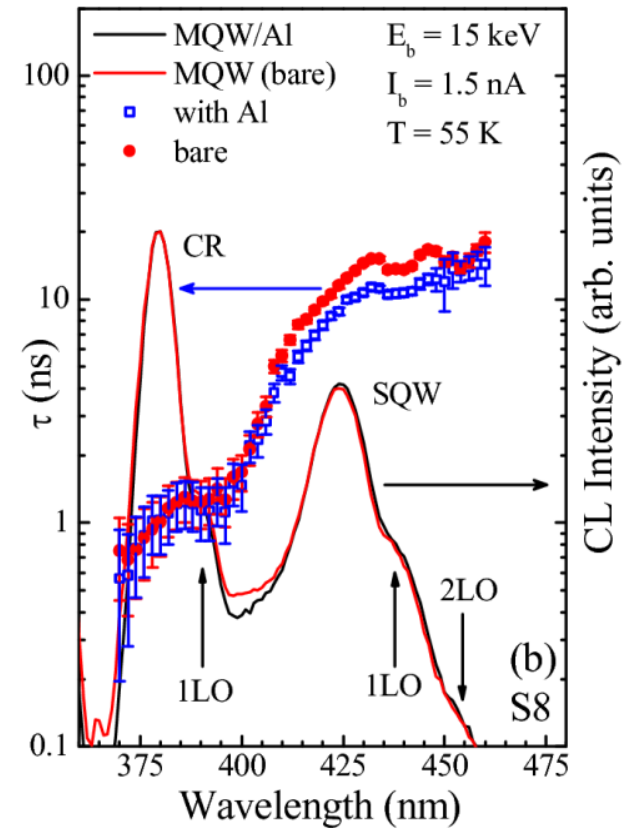
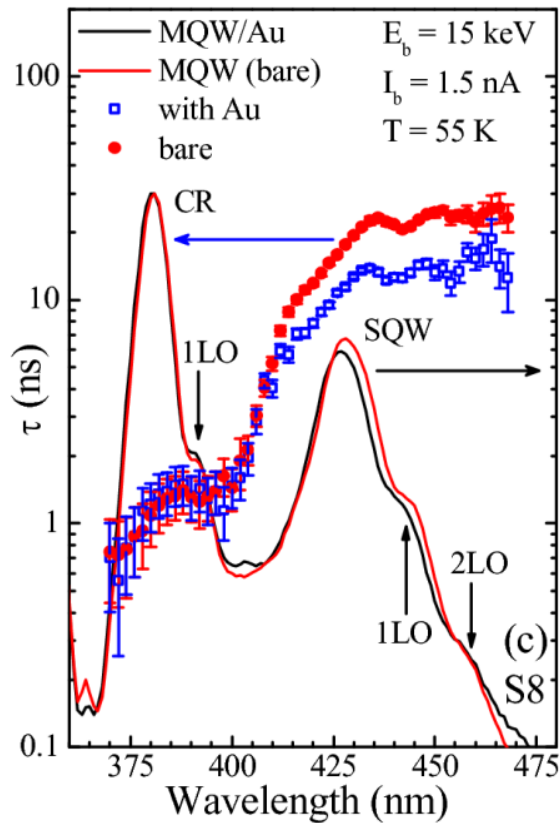
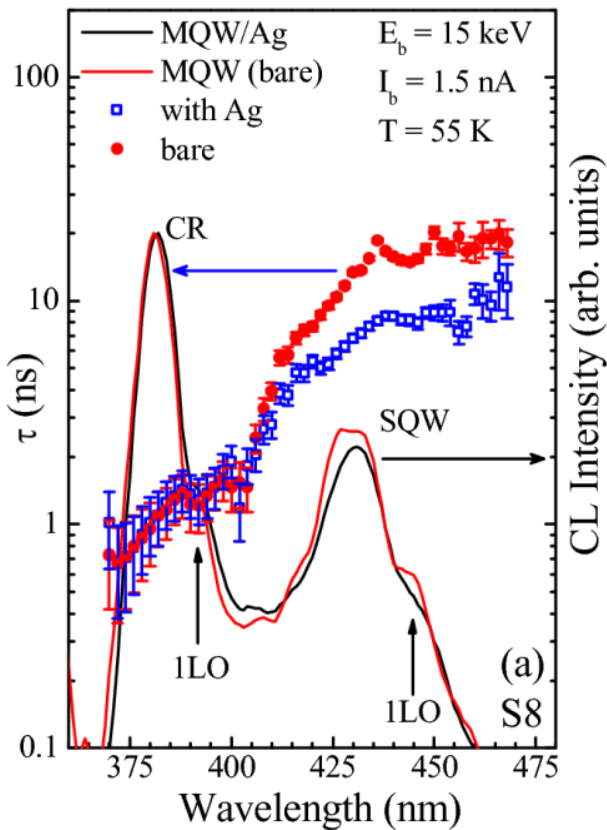
E-field and confinement potential are different for SQW and CR regions.



Time-resolved CL of bare and metal-coated InGaN/GaN QWs

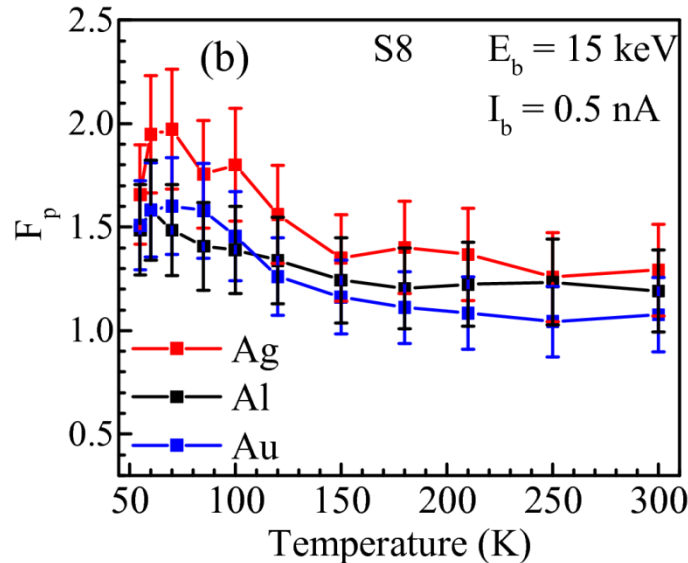
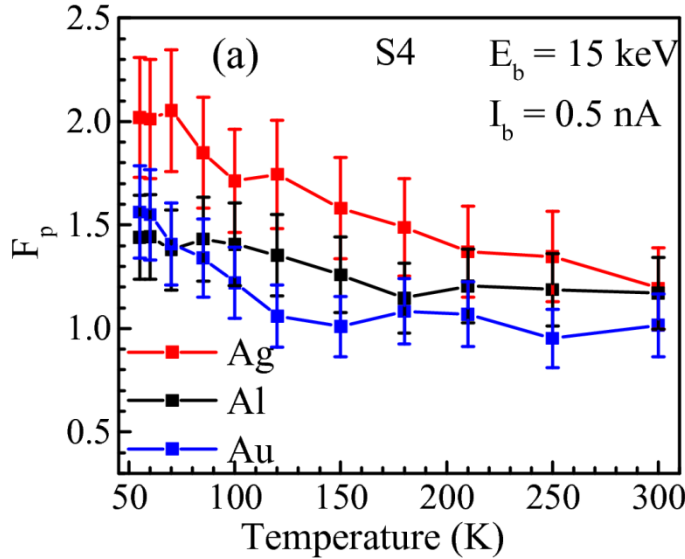
MOCVD-grown $\text{In}_x\text{Ga}_{1-x}/\text{GaN}$
MQW Samples

Metal film: Ag, Au, and Al, thickness of 20 nm
Defocused e -beam area: $\sim 1500 \mu\text{m}^2$





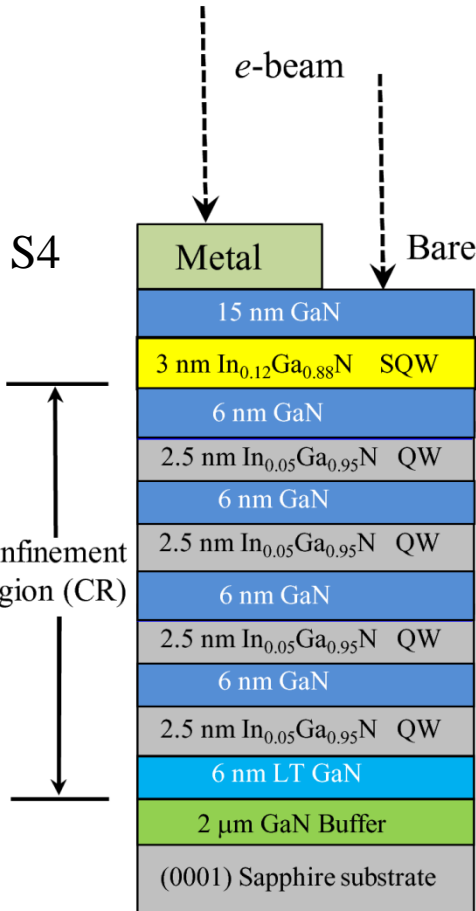
Temperature Dependence of the Purcell Factor (F_p) for the InGaN/GaN SQW



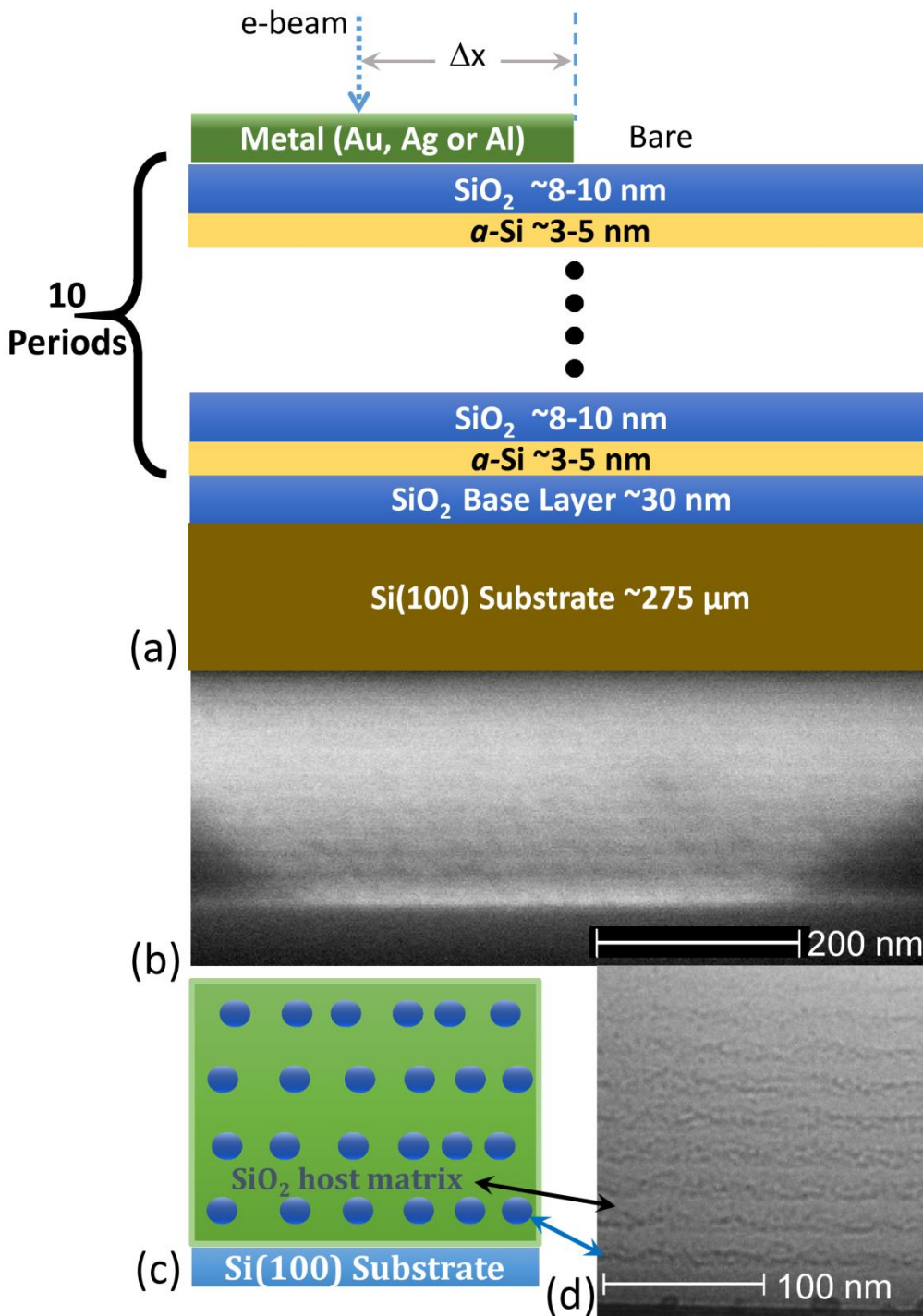
$$F_p(T) = \tau_{R(bare)} / \tau_{R(metal)}$$

The Ag film yields the largest F_p , followed by Al and Au.

Losses in the metal likely cause decrease in F_p as temp. increases.

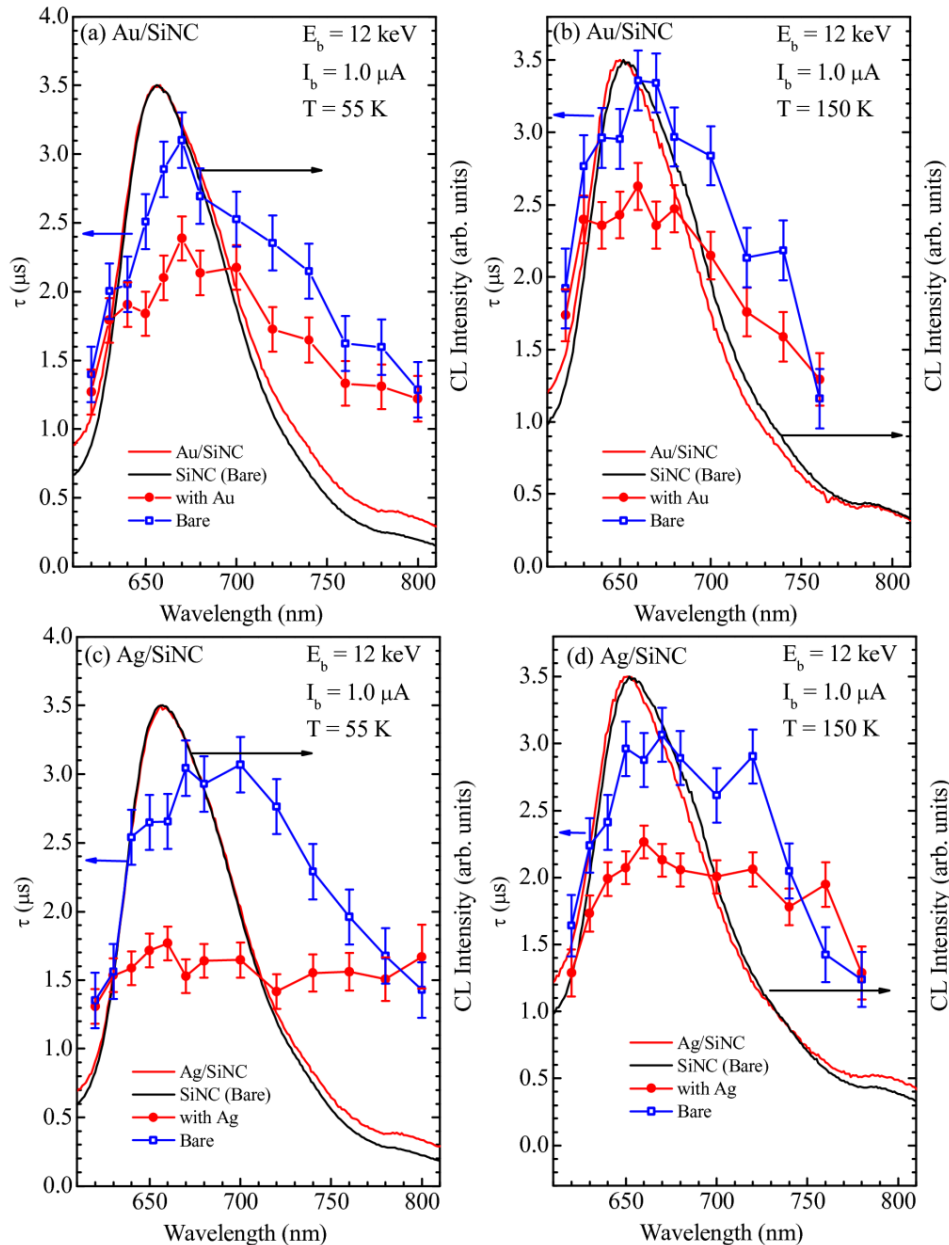


S4 – 4 QWs in the CR
S8 – 8 QWs in the CR



Enhancement in the excitonic spontaneous emission rates for Si nanocrystal (SiNC) multi-layers covered with thin films of Au, Ag, and Al

- The radiative decay rates of SiNCs are relatively small (lifetimes, τ , of $\sim 10^{-6}$ to 10^{-3} s) compared to III-V NCs ($\tau \sim 10^{-9}$ s).
- Compatibility with current Si microelectronics technology, Si LED would lead to optical interconnection applications in various stages of integrated-circuit fabrication.
- SiNCs were grown using plasma enhanced chemical vapor deposition (PECVD). Amorphous silicon ($a\text{-Si}$) and SiO_2 thin films were deposited on top of commercial $\text{Si}(100)$ wafers. The *as-grown multi-layer* sample was annealed at 1150°C for 1 hour in a N_2 flow chamber: $a\text{-Si} \rightarrow \text{SiNCs}$



The wavelength dependence of the lifetime (τ) for Au and Ag films on the SiNC sample.

Plots of τ vs λ are superimposed on plots of the CL spectra for the bare and metal-covered sample. The results are shown for temperatures of 55 and 150 K.

The peaks of the lifetime plot are shifted $\sim 10 \text{ nm}$ ($\sim 30 \text{ meV}$) towards larger λ for temperatures of 55 and 150 K, consistent with a reduced oscillator strength for larger SiNCs within the ensemble.

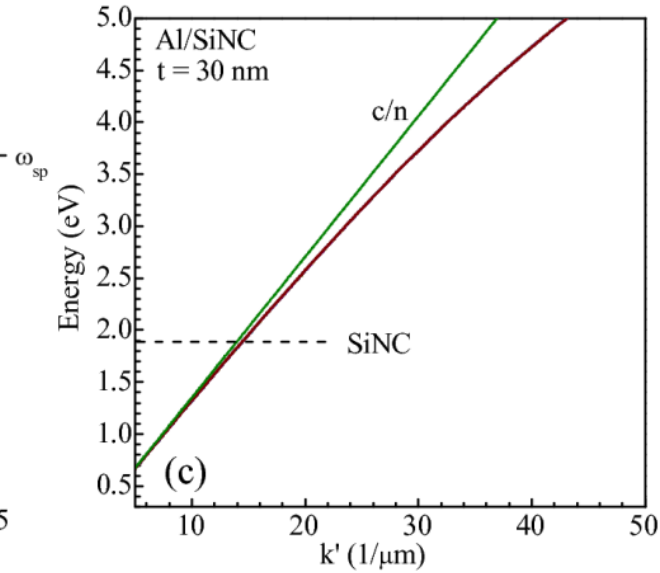
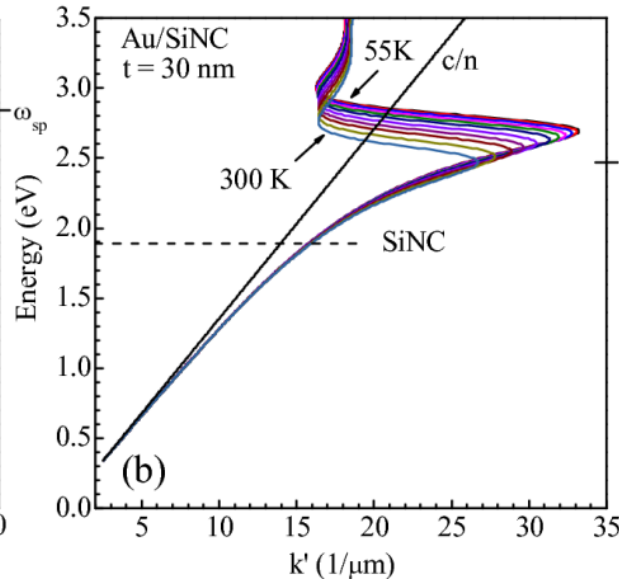
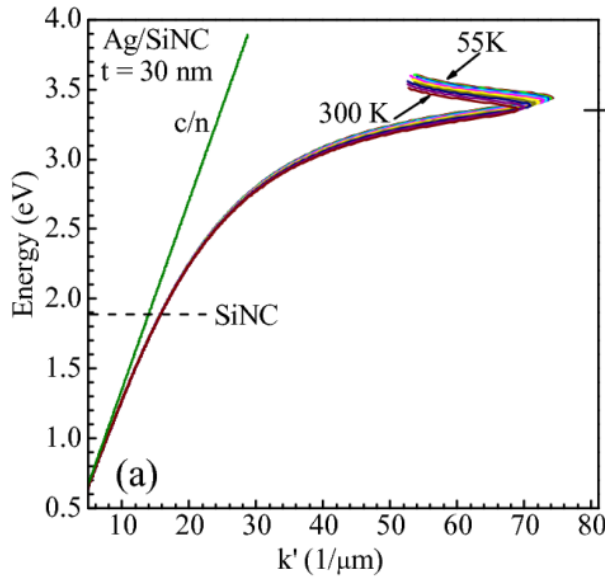
The maximum ratio (r) of the lifetimes, for which $r = \tau_{(\text{bare})} / \tau_{(\text{metal})}$, is ~ 1.4 and 2.0 at $T = 55 \text{ K}$ for the Au and Ag covered samples, respectively. Related to the energy difference between SiNC emission and ω_{sp} .



The calculated ω vs k' SPP dispersion relations for metal/SiO₂/SiNC

The method is the same as used for metal/GaN/InGaN with different $\epsilon(\omega, T)$ for SiO₂

$$\epsilon(\omega, T) = \epsilon_\infty - \frac{\omega_p(T)}{\omega^2 + i\omega\gamma(T)} + \epsilon_{CP1}(\omega, T) + \epsilon_{CP2}(\omega, T) \quad \text{For Au and Ag, as before.}$$



Numerical solutions
to the dispersion
relation:

$$\left(\frac{k_{zd}}{\epsilon_d} + \frac{k_{zm}}{\epsilon_m} \right) \left(\frac{k_{air}}{\epsilon_{air}} + \frac{k_{zm}}{\epsilon_m} \right) - \left(\frac{k_{zd}}{\epsilon_d} - \frac{k_{zm}}{\epsilon_m} \right) \left(\frac{k_{air}}{\epsilon_{air}} - \frac{k_{zm}}{\epsilon_m} \right) \exp(-2k_{zm}h) = 0$$

$$k_{zair}^2 = k_x^2 - \frac{\omega^2}{c^2} \epsilon_{air}, \quad k_{zm}^2 = k_x^2 - \frac{\omega^2}{c^2} \epsilon_m, \quad k_{zd}^2 = k_x^2 - \frac{\omega^2}{c^2} \epsilon_d$$



$$F_p(\omega, z) = 1 + \frac{\pi c^3 |E(z)|^2}{4\omega^2 \int_{-\infty}^{+\infty} u_E(\omega, z') dz'} \rho_{2D}(\omega), \quad \rho_{2D}(\omega) = \frac{1}{4\pi} \frac{\partial k^2}{\partial \omega}$$

from Fermi's Golden rule; Phys. Rev. B **60**, 11564 (1999).

For a dielectric in the transparency region (i.e., $|\varepsilon''(\omega)| \ll |\varepsilon'(\omega)|$) the energy density of the electric field in the layer is given by

$$u_E(\omega, z) = \frac{1}{8\pi} \left[\frac{\partial(\omega\varepsilon')}{\partial \omega} \right] |E(z)|^2$$

However, for metals with dissipation, the expression for the energy density is

$$u_E(\omega, z) = \frac{1}{8\pi} \left[\varepsilon' + \frac{2\omega\varepsilon''}{\gamma} \right] |E(z)|^2$$

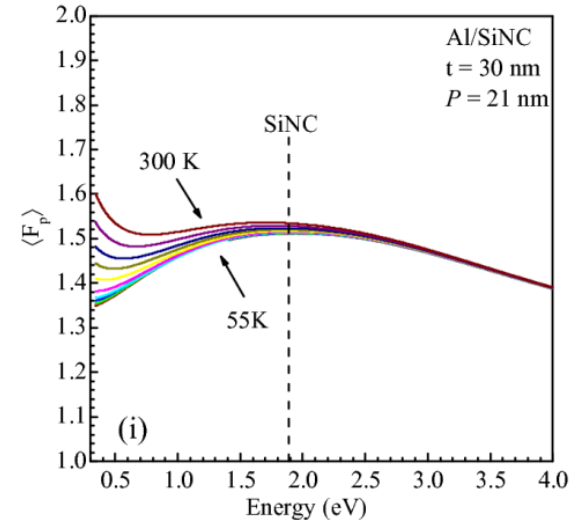
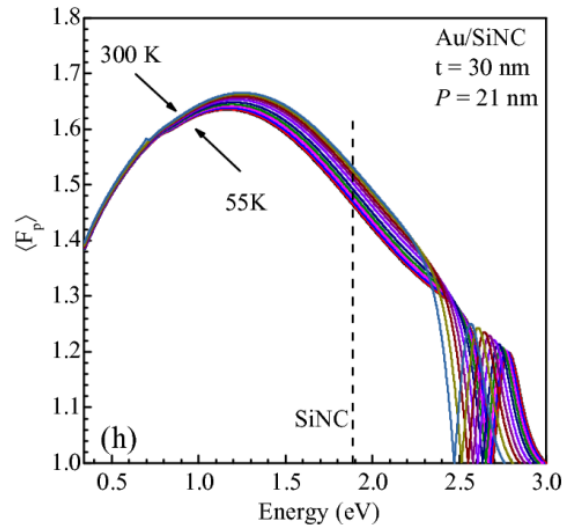
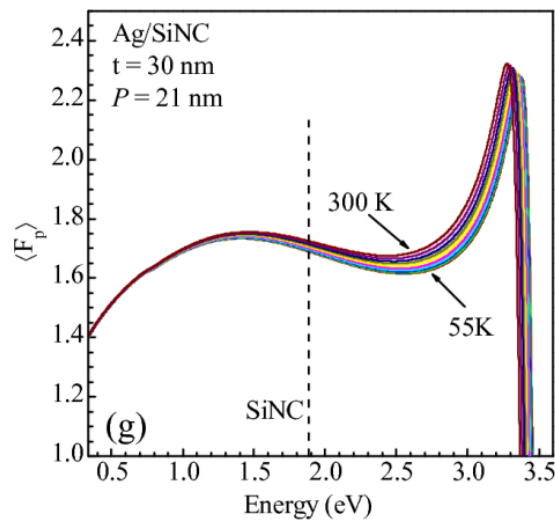
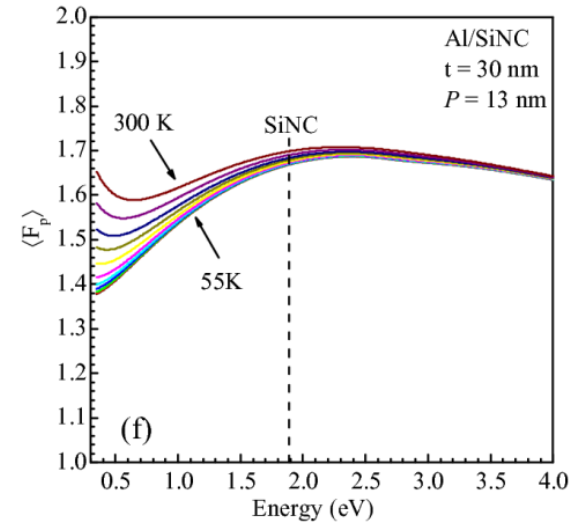
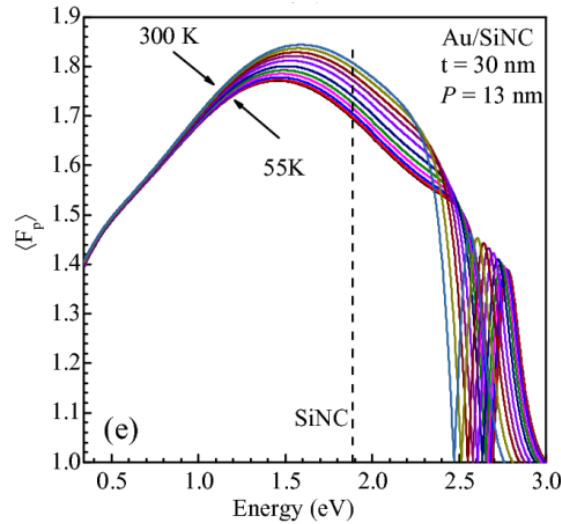
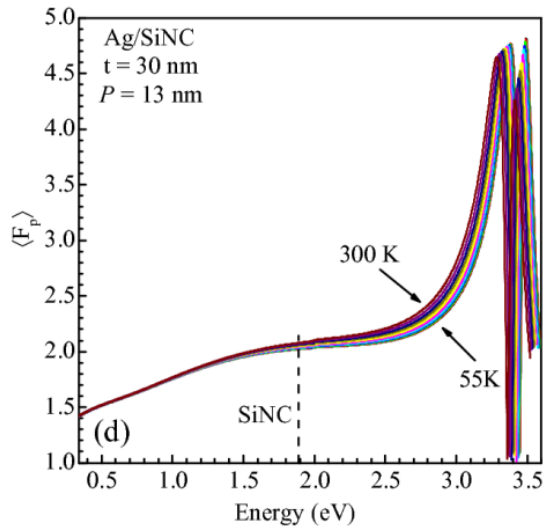
γ is the damping constant from the Drude model.

$$F_p(\omega, z) = 1 + \frac{\pi c^3 \exp(-2k_{z3}z)}{\omega^2 \left[\frac{\exp(-2k_{z2}t)}{k_{z1}} + \left(\varepsilon'_2 + \frac{2\omega\varepsilon''_2}{\gamma} \right) \left(\frac{1 - \exp(-2k_{z2}t)}{k_{z2}} \right) + \frac{\partial(\omega\varepsilon'_3)}{\partial \omega} \frac{1}{k_{z3}} \right]} \frac{\partial(k^2)}{\partial \omega}$$

$i = 1$ to 3 represent the vacuum, metal, and GaAs regions.

The calculated Average Purcell Factors $\langle F_p \rangle$ metal/SiO₂/SiNC

- $\langle F_p \rangle$ is the average of F_p over the 10-period SiO₂/SiNC structure.
- The calculations were performed for two different periodicities (P) of 13 and 21 nm.
- $\langle F_p \rangle$ is remarkably consistent with the experimental results for $r = \tau_{\text{(bare)}}/\tau_{\text{(metal)}}$, which are ~ 1.4 and 2.0 at $T = 55$ K for the Au and Ag films.





Summary

- The coupling of excitons to surface plasmon polaritons (SPPs) in metal films on GaAs/AlAs/GaAs core-shell nanowires, InGaN/GaN QWs, and Si Nano-crystals was probed using time-resolved cathodoluminescence (CL).
- Excitons were generated in the metal-coated nanostructures and QWs by injecting a pulsed high-energy electron beam through the thin metal films.
- The average Purcell enhancement factor, $\langle F_p \rangle$, was obtained by the direct measurement of the changes in the integrated NBE CL emission intensities and the temperature-dependent lifetimes.
- A model was presented for $\langle F_p \rangle$ for the three material systems, which takes into account the effects of ohmic losses of the metals and changes in the dielectric properties due to the temperature dependence of (i) the intraband behavior in the Drude model and (ii) the interband critical point transition energies which involve the d -bands of Au and Ag.



Additional information is found in our papers on this subject:

1. Y. Estrin, D. H. Rich, A. V. Kretinin, and H. Shtrikman, *Nano Letters* **13** (4), pp. 1602–1610 (2013).
2. Y. Estrin, D. H. Rich, S. Keller, and S. P. DenBaars, *Journal of Applied Physics* **117**, 043105, pp. 1-14, (2015).
3. Y. Estrin, D. H. Rich, S. Keller, and S. P. DenBaars, *Journal of Physics: Condensed Matter* **27**, 265802, pp. 1-13, (2015).
4. Y. Estrin, D. H. Rich, N. Rozenfeld, N. Arad-Vosk, A. Ron, and A. Sa'ar, *Nanotechnology* **26**, 435701 (2015).